NUMERICAL INVESTIGATION OF OFFSHORE FOUNDATION ON LIQUEFIABLE SANDS

M. R. Imansyah*, D. M. G. Taborda
Department of Civil and Environmental Engineering
IMPERIAL COLLEGE LONDON

K. W. Hau, L. Chen, R. Hosseini-Kamal
Geotechnical Engineering Department
DNV

** corresponding author: muhammad.imansyah24@imperial.ac.uk*

ABSTRACT
This study investigates the seismic response of shallow foundations resting on liquefiable sand deposits, with the aim of providing insights into the expected behaviour of Wind Turbine Installation Vessels (WTIV) when subjected to earthquake loading. A detailed calibration strategy based on commonly available ground information is outlined for Nevada sand, with a detailed characterisation of the model performance being undertaken in terms of CSR, stiffness degradation, and damping ratio curves. Subsequent validation process is also provided by simulating centrifuge experiments of footings resting on liquefiable deposits. Lastly, three-dimensional finite element analyses of a WTIV are performed employing the calibrated UBC3D-PLM parameters. The impact of soil liquefaction on the response of the WTIV is investigated, with particular emphasis given to the additional settlements caused by the seismic loading.

KEY WORDS: Wind Turbine Installation Vessel (WTIV), seismic response, soil-structure interaction, liquefaction, numerical modelling, UBC3D-PLM.

1. INTRODUCTION

Motivation of this study comes from the fact that guidelines about earthquake design of wind turbine-related constructions are less detailed compared to most other structures [1]. Given the need to expand the supply of low-carbon electricity, it is important to ensure offshore sites across the globe can be developed to explore wind energy resources. However, in many areas, such as Eastern and Southern Asia, Western America and Southern Europe, high seismic activity means that more detailed studies and standards are needed. This study focuses on the jack-up deployment, which is a pivotal sequence in offshore wind turbine construction, and how it is affected by seismic loading, particular in liquefiable sand deposits. In effect, cyclic loading due to an earthquake event in coarse-grained soil can result in a rapid pore-water pressure build-up, reducing the strength and stiffness of soil. Apart from the massive seismic loads that could be applied to the offshore structure, the severity of liquefaction-related phenomena shows the urgency of detailed research in offshore multi-hazard environments.

The main objective of this paper is to investigate the seismic response of WTIV foundations resting on liquefiable sand deposits, in order to provide insight into the expected behaviour of offshore structures when subjected to earthquake loading. To achieve this objective, a constitutive model capable of simulating the onset and development of liquefaction – UBC3D-PLM [2,3,4,5] – is first calibrated for Nevada sand using a wide range of laboratory testing data made available for the VELACS project [6].

2. UBC3D-PLM CONSTITUTIVE MODEL

It is essential to understand the UBCSAND model before exploring the UBC3D-PLM, as the former serves as the parent model of the latter. UBCSAND (University of British Columbia Sand) is a constitutive model that was originally developed by [2,3]. The main objective of this model is to simulate the liquefaction response of sands, focusing on the response of sands and silty sands with a relative density of less than about 80% [4]. UBCSAND

is an elastoplastic stress-strain model, which incorporates a hyperbolic strain-hardening rule. The current version of UBCSAND is the UBCSAND 904aR, which is also used as the basis of UBC3D-PLM of PLAXIS [5]Click or tap here to enter text..

The parameters employed in the UBC3D-PLM formulation are shown in Table 1, together with default values recommended in [5].

Table 1 Parameters of the UBC3D-PLM

Symbol	Name	Unit	Default Value
k_B^{*e}	Elastic bulk modulus number	-	-
k_G^{*e}	Elastic shear modulus number	-	-
k_G^{*p}	Plastic shear modulus number	-	-
me	Elastic bulk modulus exponent	-	0.5
ne	Elastic shear modulus exponent	-	0.5
np	Plastic shear modulus exponent	-	0.4
p_{ref}	Reference pressure	kPa	100
φ_{cv}	Constant volume angle of shearing resistance	(°)	-
φ_p	Peak angle of shearing resistance	(°)	-
c	Cohesion	kPa	0
σ_t	Tension cut-off and tensile strength	kPa	0
$(N_1)_{60}$	Corrected SPT value	-	-
R_f	Failure ratio	-	0.9
f_{dens}	Densification factor	-	1.0 (recommended)
f_{Epost}	Post-liquefaction factor	-	0.2 – 1 (recommended)

Clearly, in order to simulate liquefaction, the UBC3D-PLM model must generate excess pore water pressures when subjected to undrained shearing. This is controlled by the development of the plastic volumetric strain, which is defined in this model by a flow rule based on Rowe's stress-dilation theory, with three key observations:

- There is a given stress ratio, defined by the constant volume angle of shearing resistance, φ_{cv}, where only plastic shear strains develop, i.e. no plastic volumetric strain is generated.
- Stress ratios lower than that defined by φ_{cv} result in contractive behaviour, while for stress ratios above that value dilative behaviour takes place. This observation implies that the constant volume angle of shearing resistance operates as the phase transformation angle.
- Contraction or dilation behaviour relies on the difference between the current (or mobilised) stress ratio and the stress ratio corresponding to the constant volume angle of shearing resistance.

3. CALIBRATION METHOD

To investigate the performance of UBC3D-PLM in terms of replicating the characteristics of liquefiable sands a detailed calibration of this model was carried out for Nevada sand. This material was used in the VELACS project for which a detailed testing schedule was undertaken [6], including resonant column tests, 1D loading and unloading tests, monotonic drained and undrained triaxial tests in compression and extension, cyclic undrained triaxial tests and undrained cyclic direct shear tests. Most of these tests were carried out for samples prepared to relative densities, D_r, of 40% and 60% consolidated to various stress levels (typically 40 kPa, 80 kPa and 160 kPa). This extensive dataset makes it an important source of verification for constitutive models for sands, as they can then be used to simulate a variety of centrifuge tests performed for VELACS using the same material.

Two main challenges were encountered during the calibration of UBC3D-PLM for Nevada sand: the inability of the model to capture the effect of density meant that parameters had to be calibrated independently for the two relative densities (40% and 60%), and the fact that a wide range of tests were used forced the need to reach compromises in terms of accuracy across the entire database. The calibration was initiated by determining

parameters k_G^{*e} and ne, which control the elastic shear stiffness of the material, directly from resonant column tests. Subsequently, the constant volume angle of shearing resistance, φ_{cv}, was assumed to be given by the angle of shearing resistance at Critical State (32.7°), and therefore independent of relative density. The peak angle of shearing resistance was determined from drained triaxial constant-p compression tests, with values of 33.6° and 36.1° being obtained for D_r of 40% and 60%, respectively. The remaining parameters were established using a trial-and-error procedure based on the stress-strain behaviour measured in the undrained monotonic triaxial compressions tests. The cyclic response, in terms of stress paths and pore water pressure generation were subsequently considered. It was found that parameters controlling plasticity, such as k_G^{*p} and np, had to be modified substantially to achieve a good reproduction of the cyclic tests. The final sets of parameters are listed in Table 2 for the two relative densities tested in VELACS.

Table 2 Parameters of the UBC3D-PLM for Nevada sand (units in Table 1)

Symbol	$D_r = 40\%$	$D_r = 60\%$
k_B^{*e}	563.7	2081.9
k_G^{*e}	700.6	806.2
k_G^{*p}	200.0	1200.0
me	1.0000	0.6113
ne	0.5016	0.5416
np	0.4000	0.4000
p_{ref}	100.0	100.0
φ_{cv}	32.7	32.7
φ_p	33.6	36.1
c	0.0	0.0
σ_t	0.0	0.0
$(N_1)_{60}$	7.1	16.0
R_f	0.9	0.9
f_{dens}	0.3	0.3
f_{Epost}	0.2	0.2

To demonstrate the performance of the model after its calibration, 4 cyclic tests for a D_r of 40% are shown in Figure 1. Selected tests include two cyclic triaxial tests and two cyclic direct shear tests consolidated to two distinct stress levels. A similar selection is shown in Figure 2 for a relative density D_r of 60%. Clearly, the model is seen to reproduce the pore water pressure build up and associated reduction in effective stress with good accuracy, which is particularly impressive when the variety of tests and stress conditions are taken into account.

To verify the capabilities of the model in terms of simulating the effects of liquefaction on a footing, the centrifuge test performed by [7] is reproduced in Section 4. In this test, soil layers of Nevada sand characterised by two relative densities were used (50% and 90%). Neither match the two densities tested for the VELACS project, with two distinct approaches being employed to address this lack of experimental data. For Nevada sand with a relative density of 50%, a linear interpolation between the parameters for 40% and 60% was carried out, generating the following relationships:

$$k_G^{*e} = 528.4D_r + 489.2 \quad (1)$$

$$k_B^{*e} = 7591.2D_r - 2472.8 \quad (2)$$

$$k_G^{*p} = 5000D_r - 1800 \quad (3)$$

$$me = -1.9435D_r + 1.7774 \quad (4)$$

$$ne = 0.2D_r + 0.4216 \quad (5)$$

$$np = 0.4 \tag{6}$$

$$\sin \varphi_p = \frac{3\eta_p}{6 + \eta_p};\ \eta_p = 0.5463 D_r + 1.1386 \tag{7}$$

$$\varphi_{cv} = 32.7° \tag{8}$$

$$(N_1)_{60} = \frac{{D_r}^2}{15^2} \tag{9}$$

where D_r is the relative density between 0.4 and 0.6. For parameters not listed in the equations above, the values in Table 2 can be employed. For the layer of Nevada sand with a relative density of 90% used in the centrifuge, given that no liquefaction was observed in this material, the calibration method proposed in [8] for the HSSmall constitutive model was employed. The parameters for this material are omitted for brevity.

4. MODEL PERFORMANCE

The performance of the calibrated model was examined in two different parts: a first series of theoretical assessments, followed by the simulation of the abovementioned centrifuge tests. In terms of the first sets of studies, this investigation focused on cyclic strength (Figure 3), secant stiffness reduction curves with strain amplitude (Figure 4) and energy dissipation, quantified in this study by the damping ratio (Figure 5). Clearly, as can be seen in Figure 3, the model reproduces the effect of relative density (40%, 50% and 60%) on cyclic strength, with denser samples requiring substantially larger numbers of cycles to achieve liquefaction. This pattern is clearly seen for all tested mean effective stresses (40 kPa, 80 kPa, 160 kPa and 500 kPa). When comparing the different curves for the same relative density, the model displays the well-established trend of exhibiting lower cyclic strength for larger values of mean effective stress. These patterns, in conjunction with the reproduction of the tests observed in Figures 1 and 2 suggest that the calibrated parameters replicate the cyclic strength of Nevada sand for a wide range of densities and stress levels. In terms of stiffness reduction curves, the modelled response is compared to empirical curves [9, 10, 11] as well as that obtained using a bounding surface plasticity model [12]. In general, the model is seen to underestimate the effect of strain amplitude, with the reduction in shear stiffness taking place at larger strain amplitudes. The effect of relative density is also exaggerated when compared to expected trends: since the relative density is already included in G_{max}, it is usually considered that the normalisation of the secant shear modulus by this value is sufficient to remove the effect of density. Lastly, in terms of damping ratio, the observed trend matches those often observed in elasto-plastic models [e.g 12], with dissipated energy underestimated for small strain levels, giving place to overestimation at large strain levels when compared to empirical relationships in the literature [9, 10, 11].

With respect to the centrifuge test performed by [7], where a 6 m wide structure is embedded 1 m within a 2 m thick layer of dense Monterey sand, underlain by 3 m of Nevada sand with a relative density 50% and a deep 21 m thick layer of dense Nevada sand (90 % relative density). Two sets of results are presented in this paper, with Figure 6 showing the pore water pressure generated in the 'free-field' (here understood to denote the set of instruments located away from the structure) and Figure 7 illustrating the settlement of the structure during the application of the seismic loading. Clearly, in both cases, the model is seen to replicate the measured response with excellent accuracy.

5. NUMERICAL INVESTIGATION OF A WTIV

The numerical investigation essentially aimed to study the impact of liquefaction on a Wind Turbine Installation Vessel (WTIV) with jack-up foundations acting as the overlying structure on the seabed. The analysed problem is based on that considered in [13], with modifications introduced in terms of soil modelling to reflect the calibration described in the previous sections. The stratigraphy in the problem consists of 20 m of Nevada sand with a relative density of 60%, underlain by a 'hard layer' of Nevada sand with a relative density of 90%. The former is modelled using the calibrated UBC3D-PLM, while the latter is modelled using the HSSmall model as described above. At

the bottom of the soil deposit, a very hard rock layer was placed with a linear elastic model. All materials were modelled as undrained, assuming an at-rest coefficient of earth pressure K_0 of 0.5, with the bulk modulus of water (K_f) being 2.2 GPa. A target Rayleigh damping of 2% was used during the simulation, using as frequencies 0.5 Hz and 1.1 Hz. For the structure, the WTIV with its spudcan footings was modelled using a set of linear elastic beams and plates, including the hull, legs, and spudcan footings, as seen in Figure 8. A target Rayleigh damping of 5% was applied at the same frequencies as chosen for the soil (0.5 Hz to 1.1 Hz).

In terms of modelling seismic loading, the three components were applied at the base of the soil layers, including the horizontal motion in East-West (EW) direction, the horizontal motion in North-South (NS) direction, and the vertical or up-down (UD) direction. Lastly, in terms of boundary conditions, the boundaries of the model were placed relatively far from the structure to avoid the boundary effects in the SSI. Except for the top boundary (z-minimum), no water flow was allowed across any of the boundaries. For the dynamic boundary conditions, free-field conditions were employed in all vertical boundaries.

Figure 9 shows the excess pore water pressures generated in three alignments located at different distances from the footings (underneath the footing, adjacent to the footing, free-field) and at three different depths (top of liquefiable layer, middle of liquefiable layer and bottom of liquefiable layer). Clearly, directly under the footing, the vertical stress at the start of the earthquake loading is much higher and, as a consequence, the soil is not seen to liquefy, though this trend changes with depth, with soil liquefaction observed at the bottom of the liquefiable layer. Conversely, in the free-field, the 20 m of sand liquefy entirely under the applied earthquake loading.

The liquefaction of the top layer has dramatic effects on the response of the structure, with about 5 m settlement being estimated to occur during the seismic loading at the location of the footing. This is a consequence of the loss of bearing capacity of the material supporting the loads applied by the footings, which are considerable due to the self-weight of the WTIV and need to be redistributed. Away from the structure, in the free-field, the absence of permanent vertical loads means that the vertical displacements are considerably lower.

6. CONCLUSION

This paper investigates the use of the UBC3D-PLM model in the simulation of liquefaction-related phenomena, with a particular emphasis on the response of Wind Turbin Installation Vessels (WTIV) founded on liquefiable deposits. This study developed in several stages, the first of which included the calibration of the model based on the extensive testing dataset on Nevada sand collected during the VELACS [6] project. The model was shown to replicate a wide range of cyclic undrained tests, including triaxial tests and direct shear tests performed on samples prepared to different relative densities and initial stress levels. Subsequently, a theoretical study was conducted investigated simulated trends in terms of cyclic strength, reduction of secant shear modulus with strain amplitude and energy dissipation. Among these, the cyclic strength showed the most consistent patterns, with higher relative density and lower confining pressures leading to a larger number of cycles to liquefaction. The secant shear modulus curves indicated an excessively long ‘plateau’ prior to its reduction when compared to the empirical curves available in the literature. Finally, the energy dissipation was severely underestimated at low strain levels, with the opposite being observed for large deformations. A final verification of the model was performed by simulating a centrifuge test consisting of an isolated footing resting on a liquefiable deposit. The numerical model showed good agreement with the experimental data in terms of excess pore water pressure generated in the free-field, as well as foundation settlement due to the liquefaction of the soil layer. Based on this extensive investigation, a final study was conducted simulating a WTIV installed in a liquefiable soil. After installation, a three-dimensional ground motion was applied to simulate the seismic event, with pore pressure generation directly beneath the footing being much more limited when compared to zones further away from the footing, for which widespread liquefaction was predicted. However, pore pressure build up was still sufficiently high to lead to a reduction in bearing capacity and thus to increased settlement under the self-weight of the WTIV.

This study shows the importance of careful model calibration and validation in the modelling of complex soil-structure interaction problems such as the one considered herein. The described calibration procedure, which relies

on conventional laboratory testing, is aimed at being applicable to real design cases, although it is suggested that energy dissipation properties of the model are investigated once a final set of parameters is obtained, particularly if a very deep deposit is being simulated as there is a risk that the ground motion is excessively attenuated if strong shaking occurs. The replacement of non-liquefiable materials by alternative soil models which can better simulate damping ratio trends observed in the literature is suggested in this work as a possible approach, though more exhaustive research is required to fully assess its implications.

REFERENCES

[1] Kaynia AM Seismic considerations in design of offshore wind turbines, Soil Dynamics and Earthquake Engineering. 2019:124:399–407.

[2] Puebla H, Byrne PM, Phillips R Analysis of CANLEX liquefaction embankments: Prototype and centrifuge models, Canadian Geotechnical Journal. 1997:34(5):641–657.

[3] Beaty M, Byrne PM An Effective Stress Model for Predicting Liquefaction Behaviour of Sand, Geotechnical Earthquake Engineering and Soil Dynamics III, ASCE Geotechnical Special Publication. 1998:1(75):766–777.

[4] Beaty M, Byrne PM UBCSAND Constitutive Model Version 904aR Documentation Report. 2011.

[5] Bentley Systems, PLAXIS 3D 2024.3 Material Models Manual. 2024.

[6] Arulmoli K, Muraleetharan KK, Hossain MM, Fruth LS VELACS: Verification of liquefaction analyses by centrifuge studies - laboratory testing program and soil data report. 1992.

[7] Dashti S, Bray JD, Pestana JM, Riemer M, Wilson D Centrifuge Testing to Evaluate and Mitigate Liquefaction-Induced Building Settlement Mechanisms, Journal of Geotechnical and Geoenvironmental Engineering. 2010:136(7): 918–929.

[8] Minga E, Burd H Validation of the PLAXIS MoDeTo 1D model for dense sand. 2019.

[9] Vucetic M, Dobry R Effect of Soil Plasticity on Cyclic Response, Journal of Geotechnical Engineering. 1991:117(1): 89–107.

[10] Ishibashi I, Zhang X Unified Dynamic Shear Moduli and Damping Ratios of Sand and Clay, Soils and Foundations. 1993:33(1):182-191.

[11] Darendeli MB Development of a New Family of Normalized Modulus Reduction and Material Damping Curves, PhD Thesis, The University of Texas at Austin, Texas, 2001.

[12] Moller JK, Kontoe S, Taborda DMG, Potts DM Maximum depth of liquefaction based on fully-coupled time domain site response analysis, In: Proceedings of the 4th International Symposium on Frontiers in Offshore Geotechnics, Austin, Texas. 2020.

[13] Hau S, Barford R, Wu H, White J, Purwana O Seismic Risk Assessment and Mitigation for Wind Turbine Installation Jack-Up: A Case Study. In: Proceedings of The Jack-Up Platform Conference, London, 2023.

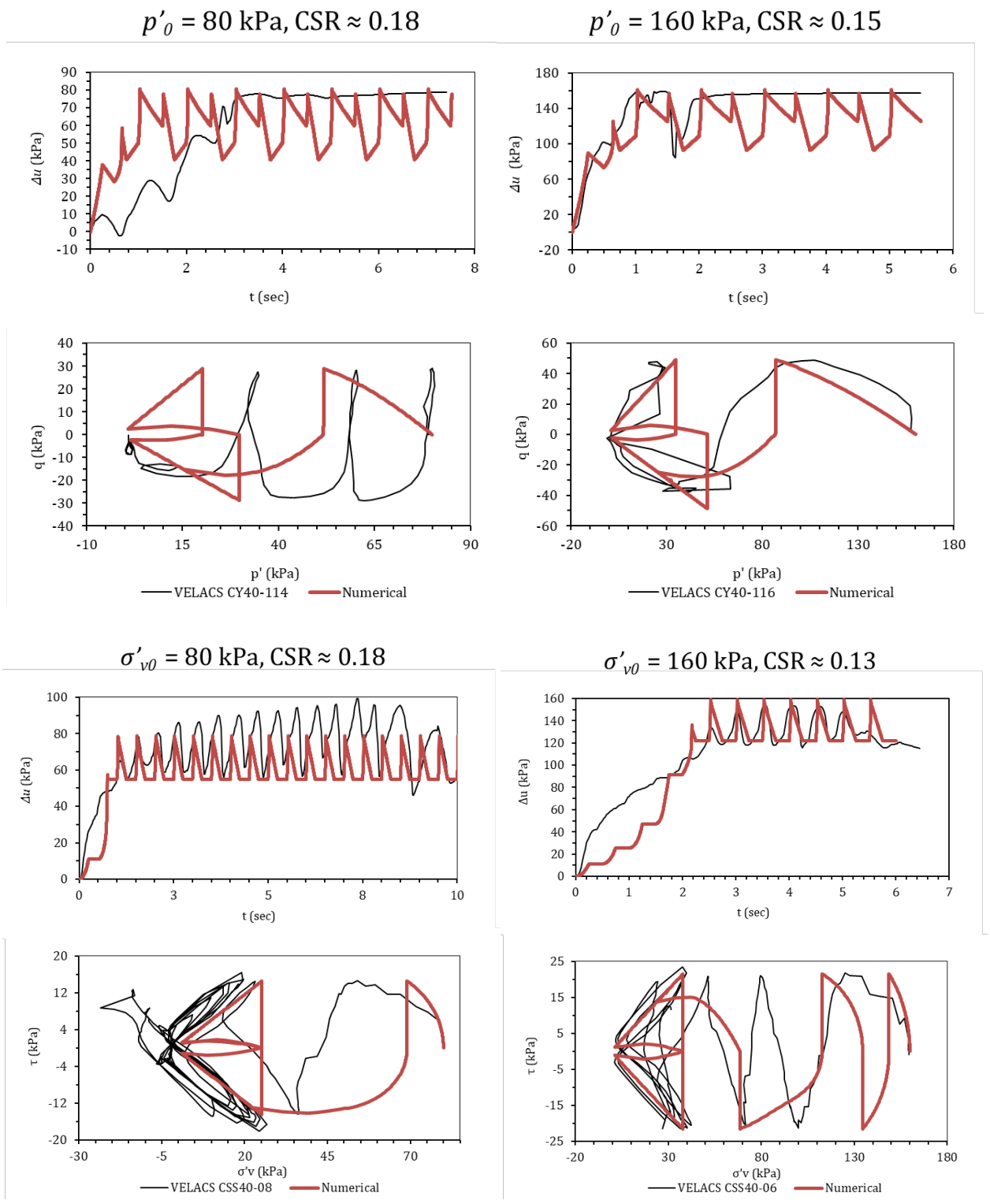

Figure 1 Comparison between measured and simulated responses for Nevada sand with D_r of 40% (top rows: cyclic undrained triaxial tests; bottom rows: cyclic undrained direct simple shear tests)

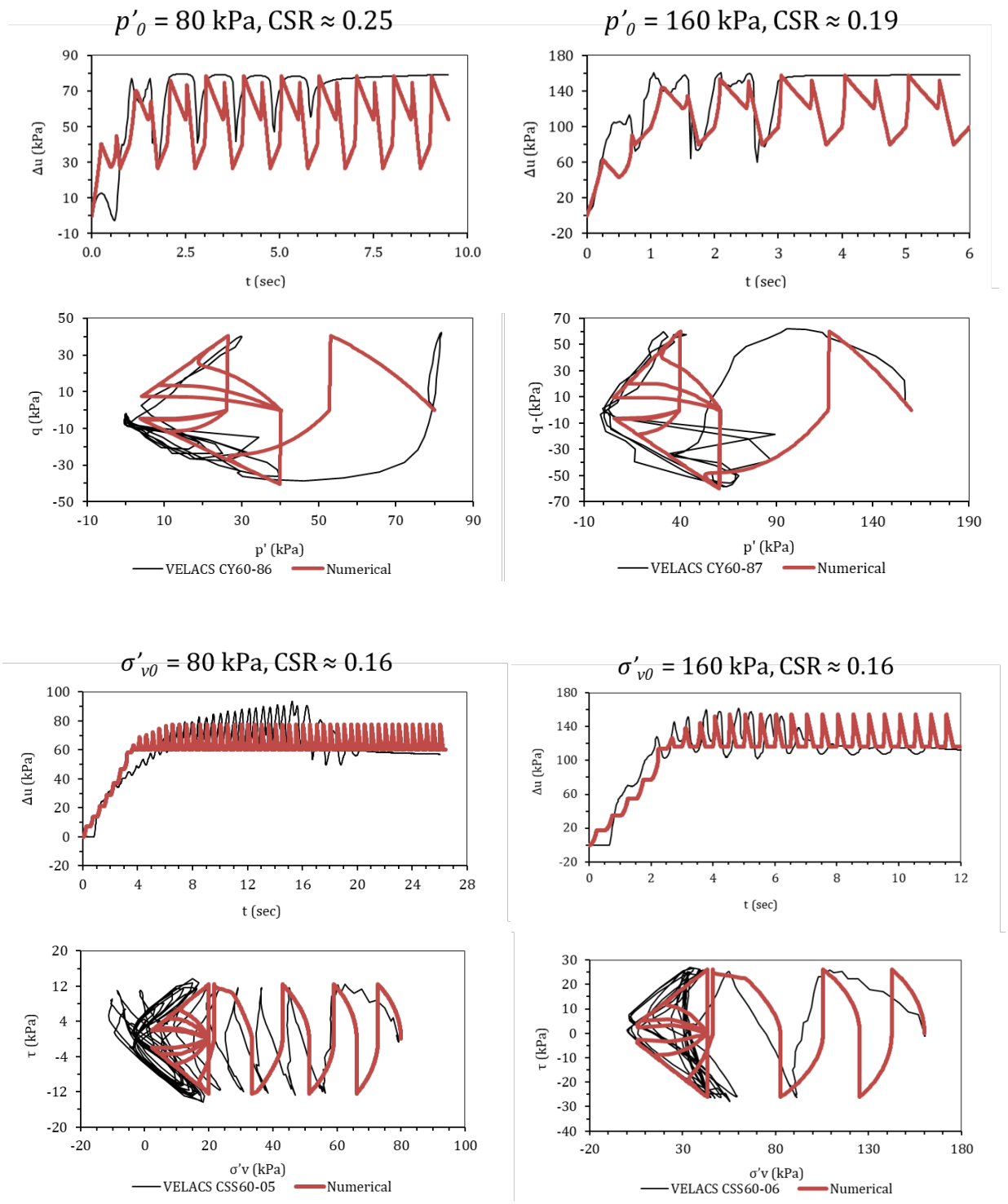

Figure 2 Comparison between measured and simulated responses for Nevada sand with D_r of 60% (top rows: cyclic undrained triaxial tests; bottom rows: cyclic undrained direct simple shear tests)

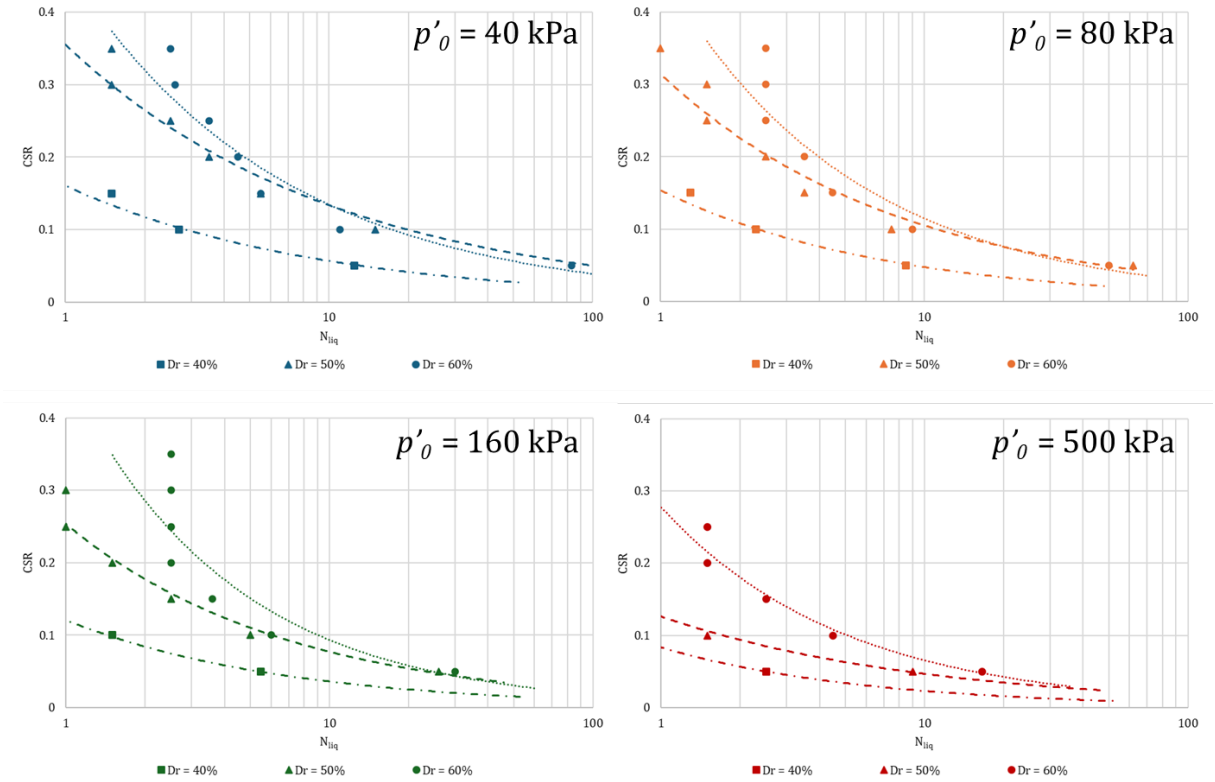

Figure 3 Simulated cyclic strength curves for Nevada sand with different initial mean effective stresses and relative densities.

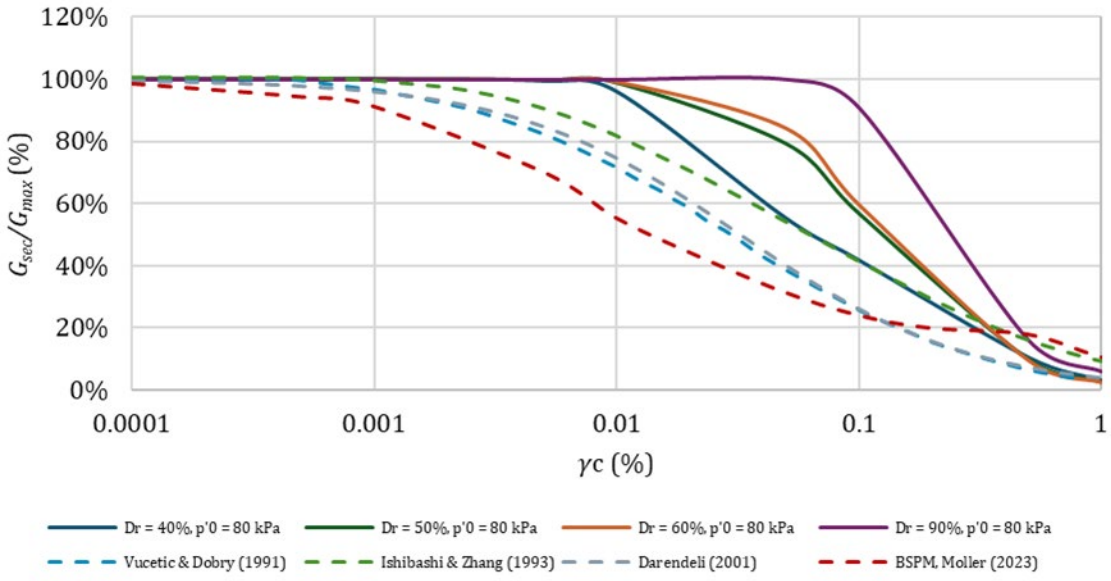

Figure 4 Simulated stiffness reduction curves compared to empirical and numerical data from the literature.

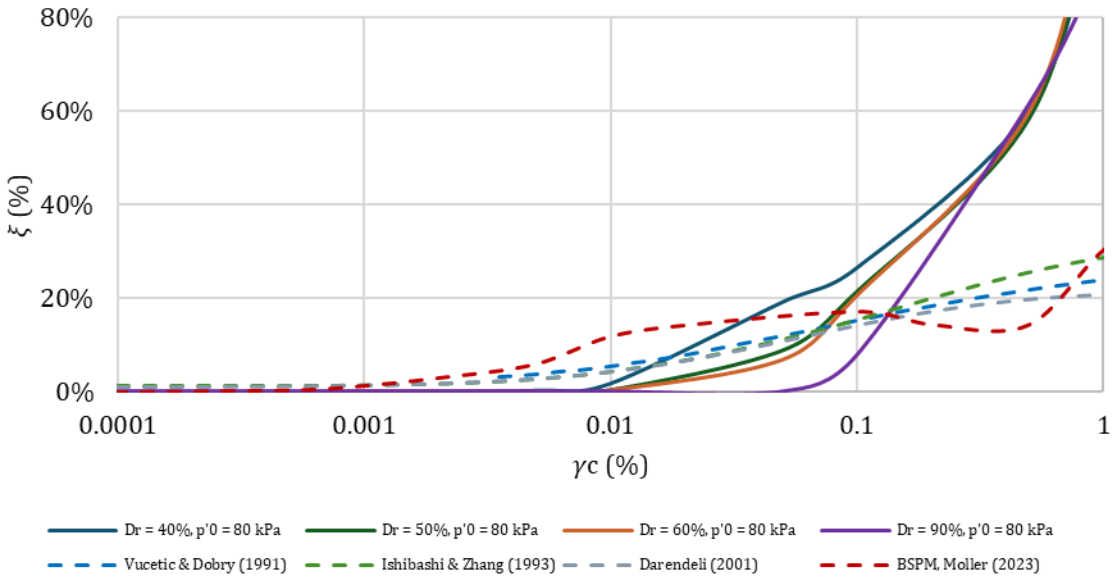

Figure 5 Simulated stiffness reduction curves compared to empirical and numerical data from the literature.

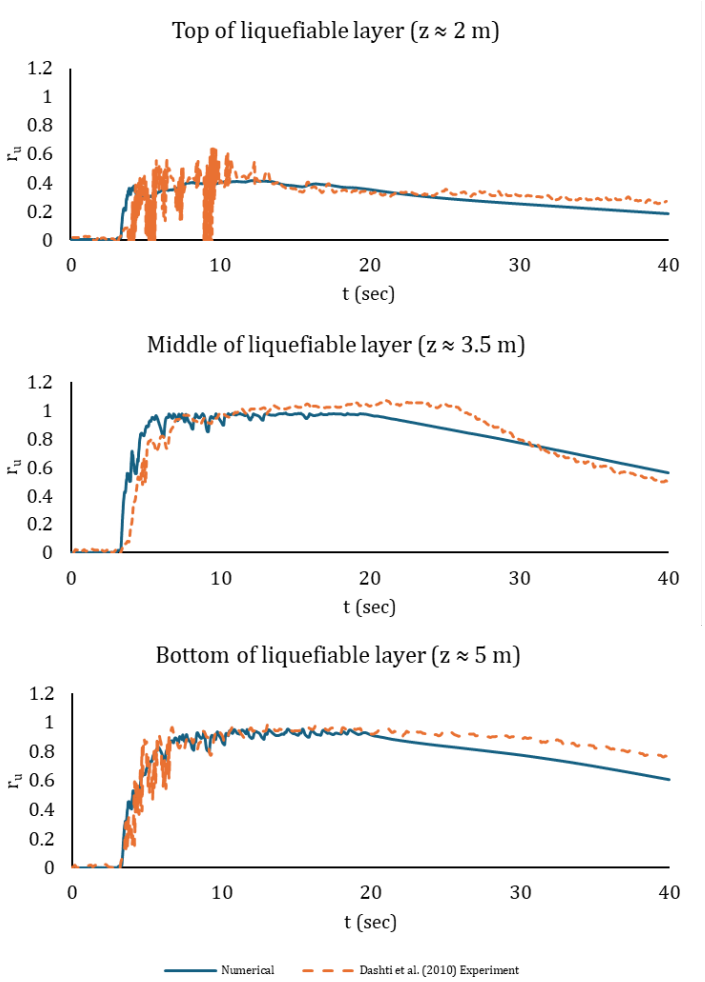

Figure 6 Modelled and measured excess pore water pressure ratios in the free field array in [7].

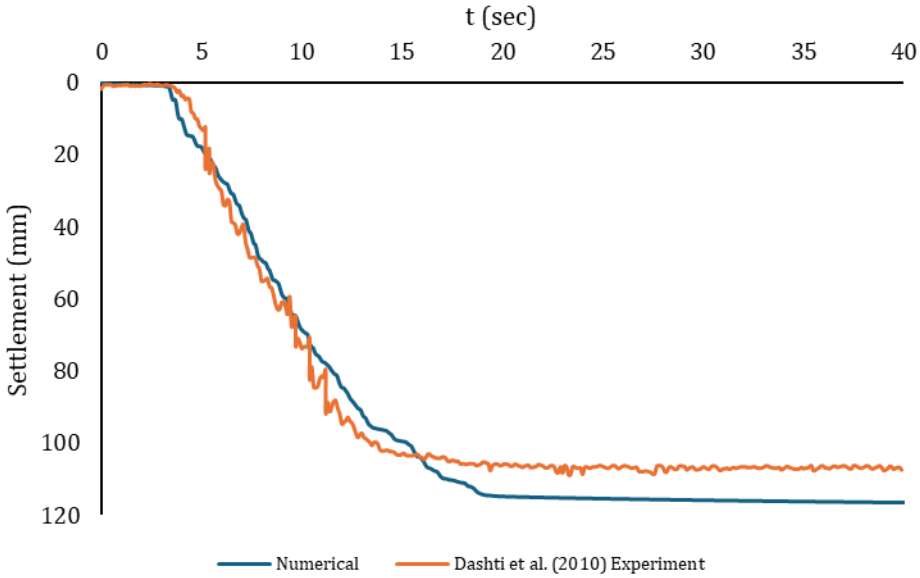

Figure 7 Modelled footing settlement compared to that measured in the centrifuge [7].

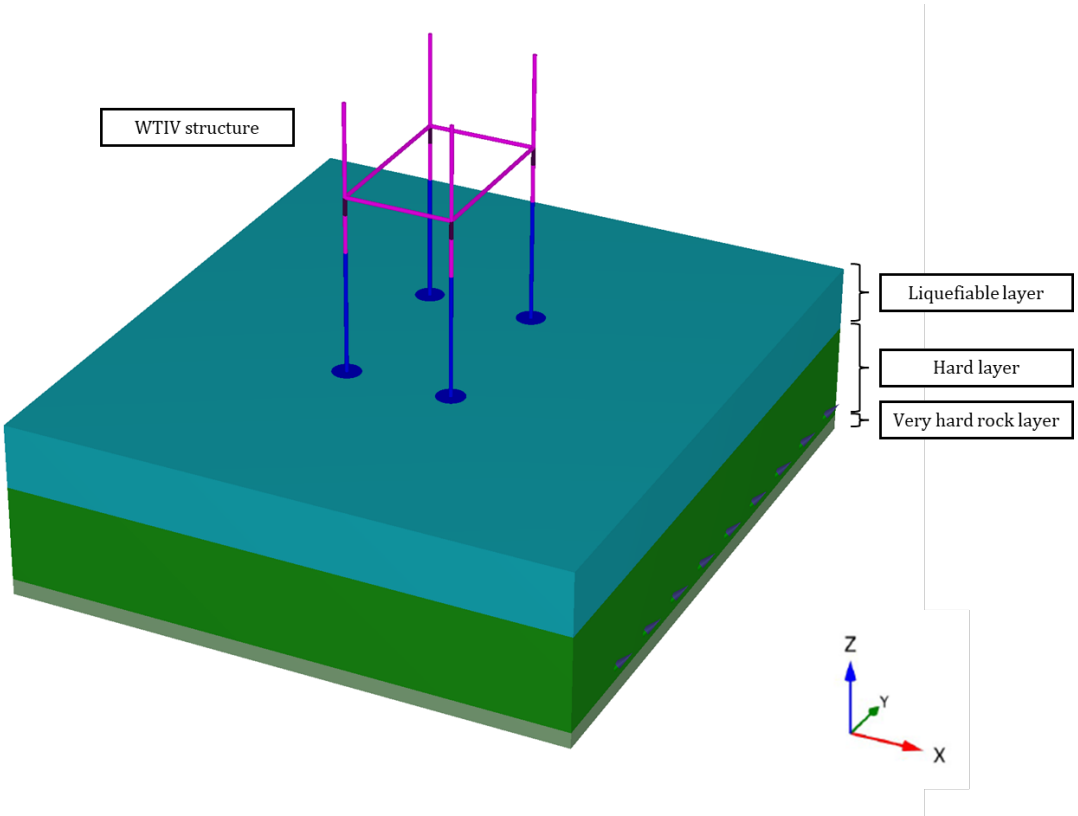

Figure 8 Numerical investigations 3D model configuration

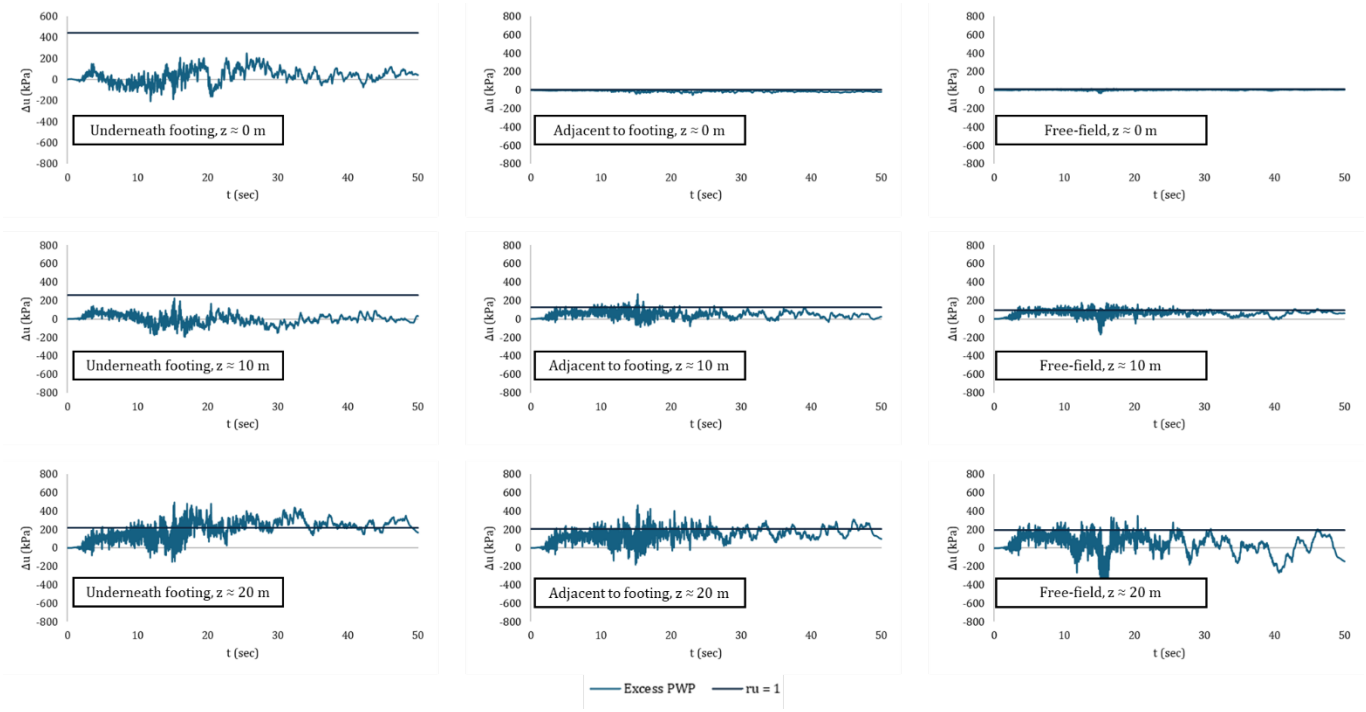

Figure 9 Excess pore water pressure time histories simulated in the WTIV problem.

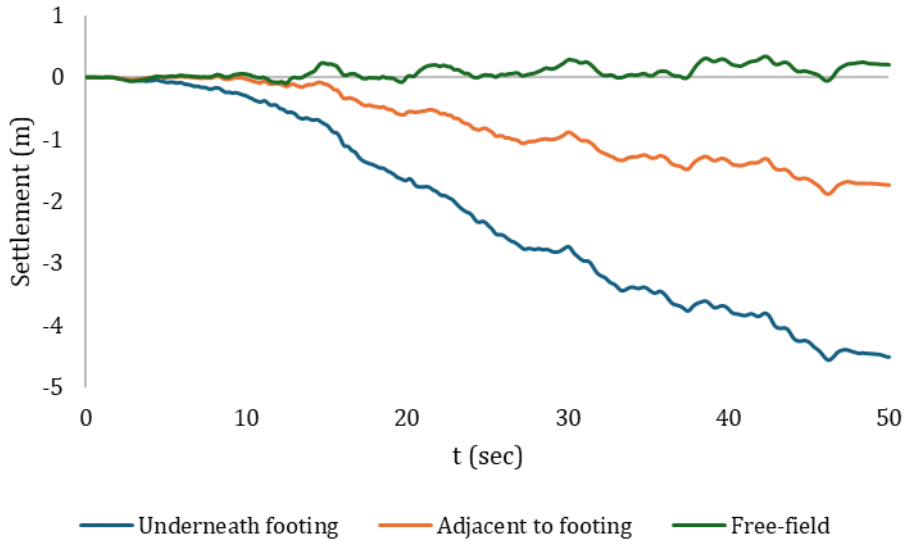

Figure 10 Settlement time histories in the WTIV problem.